

# Role of Reactive Nitrogen Species in Development of Hepatic Injury in a C57BL/6 Mouse Model of Human Granulocytic Anaplasmosis

Michelle D Browning,<sup>1,\*</sup> Justin W Garyu,<sup>1,2</sup> J Stephen Dumler,<sup>2</sup> Diana G Scorpio<sup>1</sup>

Human granulocytic anaplasmosis (HGA), caused by the granulocytic rickettsia-like organism *Anaplasma phagocytophilum*, is the 3rd most frequent vector-borne infection in North America. To understand the disease mechanisms of HGA, we developed a murine model that lacks clinical disease yet exhibits characteristic histopathologic and immunologic changes. Because the degree of hepatic histopathology is unrelated to high bacterial numbers, tissue injury in HGA is thought to occur due to products of innate immunity, such as nitric oxide (NO) and reactive nitrogen species (RNS) from cytokine-activated macrophages. To test the hypothesis that RNS cause hepatic tissue damage, mice received either water treated with a nonspecific inhibitor of inducible nitric oxide synthase, L-NAME, or untreated water for 7 to 10 d before infection and continuing thereafter. Mice were euthanized for tissue harvest at 0, 7, 14, or 21 d after infection to assess differences in histopathology, hepatic bacterial load, RNS quantity in urine and liver, and serum chemistry values. Overall, L-NAME treatment had a beneficial effect, resulting in lower histopathology scores and RNS levels compared with those of untreated mice. There were no significant differences in hepatic bacterial load among treatment groups of infected mice. The observed increases in serum glucose and alanine aminotransferase levels on day 14 appear to be unexpected side effects of L-NAME administration. HGA is best characterized as an immunopathologic disease rather than one caused by direct bacterial injury to the host. Therefore, human and animal patients with HGA likely would benefit from therapy targeting reduced inflammation to supplement anti-infective modalities.

**Abbreviations:** ALT, alanine aminotransferase; ALP, alkaline phosphatase; AST, aspartate aminotransferase; HGA, human granulocytic anaplasmosis; IFN $\gamma$ , interferon  $\gamma$ ; iNOS, inducible nitric oxide synthase; L-NAME, N<sub>o</sub>-nitro-L-arginine methyl ester hydrochloride, a nonspecific inhibitor of inducible nitric oxide synthase; NO, nitric oxide; PCR, polymerase chain reaction; RNS, reactive nitrogen species; TNF $\alpha$ , tumor necrosis factor alpha

Granulocytic anaplasmosis is a severe, potentially fatal, emerging tick-borne disease caused by *Anaplasma phagocytophilum*, a rickettsia-like organism of neutrophils that can infect humans and other mammals. Human granulocytic anaplasmosis (HGA), first recognized in 1990,<sup>2,8</sup> is the 3rd most frequent vector-borne infection in North America.<sup>12</sup> Infected patients often present with fever, myalgia, leukopenia, thrombocytopenia, and mild to moderate liver injury. Severe complications include adult respiratory distress syndrome, shock, and opportunistic infections. One discrepant observation is that the degree of disease and histopathology in tissues does not correlate with the low quantities of organisms in peripheral blood neutrophils.<sup>23,29,30</sup>

To understand the disease mechanisms in HGA, we developed a murine model.<sup>7,22,23,29</sup> In this system, immunocompetent mice never develop overt clinical disease but they generate high levels of plasma interferon  $\gamma$  (IFN $\gamma$ ) and generally exhibit clearance of the organism within 21 d. Despite the lack of clinical signs, the model is useful because histopathologic and cytokine responses are similar to those of humans and animals with clinical signs.<sup>11,18</sup> Moreover, in the mouse model there is a close association between the pro-

duction of IFN $\gamma$  and the degree of hepatic histopathology,<sup>23</sup> even in the absence of increased pathogen load. This pattern suggests that tissue injury occurs via generation of nitric oxide (NO) and reactive nitrogen species (RNS) from cytokine-activated macrophages.<sup>3</sup> Therefore, we hypothesized that hepatic histopathology and injury in *A. phagocytophilum*-infected C57BL/6 mice results from increased production of RNS. To prove this hypothesis, we studied hepatic histopathology, clinical chemistry, RNS production, and bacterial load associated with *A. phagocytophilum* infection in mice. We also aimed to verify the effects of RNS in vivo by use of a nonspecific inhibitor of inducible nitric oxide synthase (iNOS).

## Materials and Methods

**Animals.** C57BL/6 mice were obtained from Jackson Labs (Bar Harbor, ME) at 4 to 6 wk of age and were maintained in a barrier facility. These mice were negative for *Helicobacter* spp. and tested negative by sentinel evaluation for mouse adenovirus, ectromelia virus, mouse rotavirus, mouse encephalomyelitis virus strain GD-VII, lymphocytic choriomeningitis virus, mouse hepatitis virus, *Mycoplasma pulmonis*, pneumonia virus of mice, reovirus, Sendai virus, mouse parvovirus, minute virus of mice, endoparasites, and ectoparasites. Mice were maintained in autoclaved ventilated rack caging (Allentown Caging Equipment, Allentown, PA) with acidified water and autoclaved diet (Harlan Teklad 2018S, India-

Received: 6 Oct 2005. Revision requested: 21 Nov 2005. Accepted: 23 Nov 2005.

<sup>1</sup>Department of Comparative Medicine and <sup>2</sup>Department of Pathology, The Johns Hopkins University School of Medicine, Baltimore, Maryland.

\*Corresponding author. Email: mbrowni5@jhmi.edu

**Table 1.** Experimental design grouped by water treatment and infection status of C57BL/6 mice. Mice from each group were euthanized for tissue harvest at time points 0, 7, 14, and 21 days post-inoculation

Treatment	Inoculum
None	Uninfected HL60 cells
L-NAME	Uninfected HL60 cells
None	<i>A. phagocytophilum</i> -infected HL60 cells
L-NAME	<i>A. phagocytophilum</i> -infected HL60 cells

napolis, IN). Mice were inoculated intraperitoneally with either uninfected or *A. phagocytophilum*-infected HL-60 cells on day 0. Mice were euthanized with CO<sub>2</sub>, and samples were harvested on day 0, 7, 14, or 21. A 2nd cohort was studied later to determine reproducibility of results. Mice received either untreated water or water treated with 1 mg/ml of the NOS inhibitor N<sup>ω</sup>-nitro-L-arginine methyl ester hydrochloride (L-NAME). There were 3 to 4 animals per time point in each treatment group (Table 1). One additional animal per group was examined on day 0 prior to inoculation to establish baseline effects of L-NAME on histopathology and to verify the absence of concurrent disease. Animals were observed daily by a veterinarian and were monitored for signs of infection or distress, including loss of appetite, dehydration, rough hair coat, weight loss, dyspnea, decreased activity, and lack of interaction with cagemates. All procedures and experiments were approved by The Johns Hopkins University Animal Care and Use Committee, and mice were maintained in facilities that adhered to housing guidelines as outlined in the *Guide for the Care and Use of Laboratory Animals*.<sup>24</sup>

**Cell lines.** The HL-60 promyelocytic cell line was used as the in vitro host cell for *A. phagocytophilum* and was maintained in RPMI 1640 culture media supplemented with 5% fetal bovine serum and 2 mM L-glutamine at 37 °C in a 5% CO<sub>2</sub> environment. Raw 264.7 cells were grown in Dulbecco Modified Eagle Medium (DMEM) without phenol red and were supplemented with 10% fetal bovine serum, 2 mM L-glutamine, and 1% penicillin–streptomycin at 37 °C in a 5% CO<sub>2</sub> environment until confluent. This cell line, when stimulated with 10 µg/ml lipopolysaccharide for 24 h, causes release of NO and was used as a positive control for the Griess reagent assay.

**Preparation of *A. phagocytophilum*.** *A. phagocytophilum* (Webster strain, passage 10) was propagated in HL-60 cells in RPMI 1640 medium with 2 mM L-glutamine and 1% to 5% fetal bovine serum at 37 °C in 5% CO<sub>2</sub>. Once HL-60 cells had reached an infection rate of 80%, cells were pelleted at 400 × g for 10 min and resuspended in 400 µl RPMI 1640 medium for a total of 1 × 10<sup>6</sup> *A. phagocytophilum*-infected cells. An equivalent number of uninfected HL-60 cells were used as an inoculum for control mice.

**NO inhibition.** Mice were treated with 1 mg/ml L-NAME (Sigma, St Louis, MO) in sterile double-distilled water, which was changed every 2 to 3 d during the initial experiment and daily for 5 consecutive days per week (Monday through Friday) for the 2nd cohort of mice in the replicate experiment. Dosing frequency initially was determined in light of literature searches and discussions with JHU colleagues studying NO inhibition.<sup>21</sup> The dosing regimen then was amended to more frequent replacement of water after consultation with Sigma regarding the stability of L-NAME in water beyond 24 h. Treated mice had continuous access to L-NAME, and an equal number of controls received untreated water for the entire duration of the study. Treatment with L-NAME was instituted 7 to 10 d before the beginning of the experiment to ensure that inhibition was initiated adequately by the time of infection.

**Table 2.** Semiquantitative scoring system for hepatic histopathology

Hepatocyte damage	1	Apoptosis and degeneration of individual hepatocytes
	2	Clusters or small aggregates of apoptotic hepatocytes
	3	Medium to large areas of apoptotic hepatocytes
	4	Large areas of hepatocyte apoptosis or necrosis
Frequency of lesions	1	0 or 1 lesion at 400×
	2	1 to 5 lesions at 400×
	3	5 to 10 lesions at 400×
	4	>10 lesions at 400×
Size of inflammatory lesions	1	Small infiltrates with few inflammatory cells
	2	Medium-sized infiltrates with small to moderate numbers of inflammatory cells
	3	Large infiltrates with moderate to large numbers of inflammatory cells
	4	Extensive infiltration with large numbers of inflammatory cells
Extent of perivascular inflammation	1	Occasional inflammatory infiltrates at vessel walls
	2	10% to 40% of triad vessels affected and cuffing of ≤3 cells in thickness
	3	40% to 70% of triad vessels affected and cuffing of 4 to 7 cells in thickness
	4	>70% of triad vessels affected and cuffing of >7 cells in thickness

Liver sections were evaluated by two reviewers in a blinded fashion and then scored independently according to the four parameters above.

**Hepatic histopathology.** At necropsy, liver and spleen were harvested and fixed in 10% neutral-buffered formalin, embedded in paraffin, sectioned, and stained with hematoxylin and eosin. Histologic sections were scored blinded and graded with a semiquantitative scoring system modified from Olano and colleagues.<sup>25</sup> Liver lesions were assessed according to 4 parameters: hepatocyte damage; frequency of lesions; size of inflammatory lesions; and extent of perivascular inflammation (Table 2). Each parameter was independently assigned a score of 0 (no pathology) to 4, and the scores were added to yield a total liver pathology score for a minimum of 0 and a maximum of 16. All hepatic histopathology scores were then ranked against each other, a median HL-60 background rank from each control group was calculated and subtracted from each mouse in the paired infected group, and then all infected animals ranked again to achieve a final order of decreasing severity. This method of ranking was used to ensure that subtle differences could be resolved among groups of mice with similar scores.

**Measurement of bacterial DNA quantity.** Samples obtained from mice inoculated with infected HL-60 cells from the replicate experiment were tested for *A. phagocytophilum* DNA by quantitative polymerase chain reaction (PCR) amplification. Briefly, liver sections from each mouse were trimmed to 20- to 25-mg pieces, and total nucleic acids were prepared using the Qiagen DNA Mini Extraction Kit (Qiagen, Valencia, CA). Total mammalian and bacterial DNA was quantified, and approximately 20 ng was used per 25-µl PCR reaction in a 96-well plate format. A standard curve was incorporated with each plate by using a beginning concentration of 1 × 10<sup>4</sup> *A. phagocytophilum*-infected HL-60 cells/µl, with 10-fold dilutions through 1 × 10<sup>-2</sup> infected cells/µl. Amplification reactions were performed on an automated analyzer (IQ5, Bio-Rad, Hercules, CA). The TaqMan reporter probe, primer sequences, and amplification conditions were used as previously reported.<sup>29</sup> Results are expressed as the number of *A. phagocytophilum*-infected cells/20 ng host liver DNA.

**Measurement of RNS in mouse liver and urine.** We treated 40 to 60 mg of mouse liver with twice the equivalent volume of collage-

nase (lyophilized, Invitrogen, Carlsbad, CA) solution containing 3 mM  $\text{CaCl}_2$  for 60 min under gentle agitation at 37 °C. Collagenase was prepared from frozen stocks diluted 1:10 with Hanks buffered salt solution (working solution, 21 mg/ml). Samples then were sonicated until tissue was completely disrupted. Liver homogenates then were spun at  $13,000 \times g$  for 10 min and the supernatant collected for further processing. To measure the amount of nitrite and nitrate, samples were diluted with an equal volume of Hanks balanced salt solution and filtered through 10-kDa Microcon filters (Millipore, Billerica, MA). By using a colorimetric assay kit based on the Griess reagent assay (Cayman Chemicals, Ann Arbor, MI), nitrite and nitrate levels were quantified from a standard curve, and values were expressed in  $\mu\text{M}$  per equivalent mass:volume ratio of liver. Raw 264.7 cells were used as the positive control. Urine was collected either by free catch during restraint or from a mouse transport box and was pooled within groups in some cases if small volumes of urine were voided. Determination of urine nitrate and nitrite concentrations was performed using the kit described earlier, except urine (diluted 1:20 to 1:80 in Hanks solution) was placed directly into the assay after brief centrifugation of samples to pellet particulate matter.

**Serum clinical chemistry.** Approximately 100  $\mu\text{l}$  blood was placed in a serum separator tube and centrifuged to obtain serum. Complete serum biochemistry was performed on mice euthanized on days 7 and 14 only. Analysis was performed predominantly for values of alanine aminotransferase (ALT), aspartate aminotransferase (AST), alkaline phosphatase (ALP), and glucose. Samples were sent to an outside animal health laboratory for analysis (Antech Diagnostics, Lake Success, NY).

**Data analysis.** For ranked histopathologic data, the nonparametric Mann–Whitney test for unpaired groups was performed to assess differences associated with NOS inhibition and time after infection, and results were expressed as median ranks. Unpaired two-tailed *t* tests were used to evaluate differences among groups of mice for the following parameters: concentration of NO in urine or liver tissue; hepatic ehrlichial burden; and serum clinical chemistry. These results were expressed as mean  $\pm$  standard error of the mean. Welch correction was used when groups had unequal variances (F test). Pearson or Spearman (for ranked data) correlation analysis was performed across all variables. Graph Pad Prism 4 (San Diego, CA) statistical graphing software was used for all statistical analyses. Results were considered statistically significant when  $P < 0.05$ , and trends were considered to be present when  $0.05 < P < 0.10$ .

## Results

**Hepatic histopathology.** Total liver scores ranged from 3 to 9, with infrequent scores of 4 in any single category. Figure 1 represents a sample of histologic scores from each category. Day 0 uninoculated mice had only occasional, small inflammatory lesions (total pathology scores of 4.5 and 3 for L-NAME-treated and untreated mice, respectively), indicating negligible background pathology. Overall, for the preliminary experiment (Figure 2), there was a decreasing rank score for both L-NAME-treated and untreated mice. L-NAME-treated mice continued this reduction in rank score through day 21, whereas untreated mice had an increase in hepatic injury and reached peak pathology at day 21. There were no significant differences in rank scores between treated and untreated groups on days 7 or 14. Untreated mice had a trend ( $P = 0.10$ ) toward higher pathology rank on day 21 compared with L-NAME treated mice (median, 20 and 2, respectively).

For the replicate experiment (Figure 3), mice receiving untreated water had nearly significant ( $P = 0.0571$ ) increasing rank score between day 7 (median, 10) and day 14 (median, 17) at peak pathology and return to day 7 levels by day 21. L-NAME-treated mice had nearly significant ( $P = 0.0571$ ) decreasing rank scores between days 7 (median, 15) and 14 (median, 1), which remained essentially unchanged through day 21. On day 7, L-NAME-treated mice (median, 15) had nearly significant ( $P = 0.0571$ ) higher rank scores than untreated mice (median, 10). At day 14, the trend was opposite, with untreated mice (median, 17) having nearly significant ( $P = 0.0571$ ) higher rank scores than L-NAME-treated mice (median, 1). Hepatic histopathology did not significantly correlate with any of the other studied parameters.

**A. phagocytophilum hepatic DNA quantity.** There were no significant differences in bacterial DNA load measured between matched groups at any time point, and quantities of infected cells did not correlate with the degree of histopathology or treatment group. There was no effect of NOS inhibition on bacterial numbers detected in liver samples. Overall, bacterial loads among all mice reached a maximum of about 3 infected cells/20 ng host DNA on day 7 as extrapolated from the standard curve. By day 21, *A. phagocytophilum*-infected cells were no longer detected in most animals. Animals inoculated with uninfected HL-60 cells were negative by quantitative PCR.

**Measurement of RNS in mouse liver and urine (Table 3).** Measurements of RNS in liver supernatants were significantly ( $P = 0.0046$ ) higher on day 14 of the replicate experiment for all animals on untreated water compared with L-NAME-treated animals, regardless of infection status (Figure 4). This difference also was noted between treated and untreated day 14 mice infected with *A. phagocytophilum* ( $P = 0.0215$ ). Differences in quantity of RNS from urine were similar for day 14 mice, with untreated animals having a significantly ( $P = 0.0124$ ) higher urine RNS compared with L-NAME-treated mice, regardless of infection status (Figure 5). This difference also was noted for infected mice, with a trend ( $P = 0.0836$ ) toward a greater quantity of urine RNS in untreated mice compared with L-NAME-treated mice. This difference continued through day 21, with a trend ( $P = 0.0885$ ) toward higher urine RNS quantity in untreated mice compared with L-NAME-treated mice. Urine and liver RNS levels did not correlate significantly with hepatic histopathology, bacterial load, or serum chemistry, nor did they correlate with each other.

**Serum clinical chemistry.** There were no significant differences between mice with regard to serum clinical chemistry parameters on day 7. On day 14 of the replicate experiment, however, mice treated with L-NAME varied significantly ( $P < 0.05$ ) from untreated mice, regardless of infection status, with regard to select serum chemistry parameters (Table 4). These data were chosen for analysis to assess the effects of NOS inhibition on serum biochemical markers. Day 14 glucose values were significantly ( $P = 0.0412$ ) higher in L-NAME-treated mice than in untreated animals. Day 14 ALT values were nearly significant ( $P = 0.0531$ ), with L-NAME-treated mice having higher ALT levels than untreated mice. There were no significant differences in AST or ALP values among animals. ALT and AST values generally were elevated 5 to 10 times the normal values in mice. This pattern was found among uninfected and infected mice in both treatment groups, although there were no statistically significant differences detected between groups. Serum chemistry parameters did not significantly correlate with histopathology, bacterial load, or liver or urine RNS levels. These findings were evident in the replicate

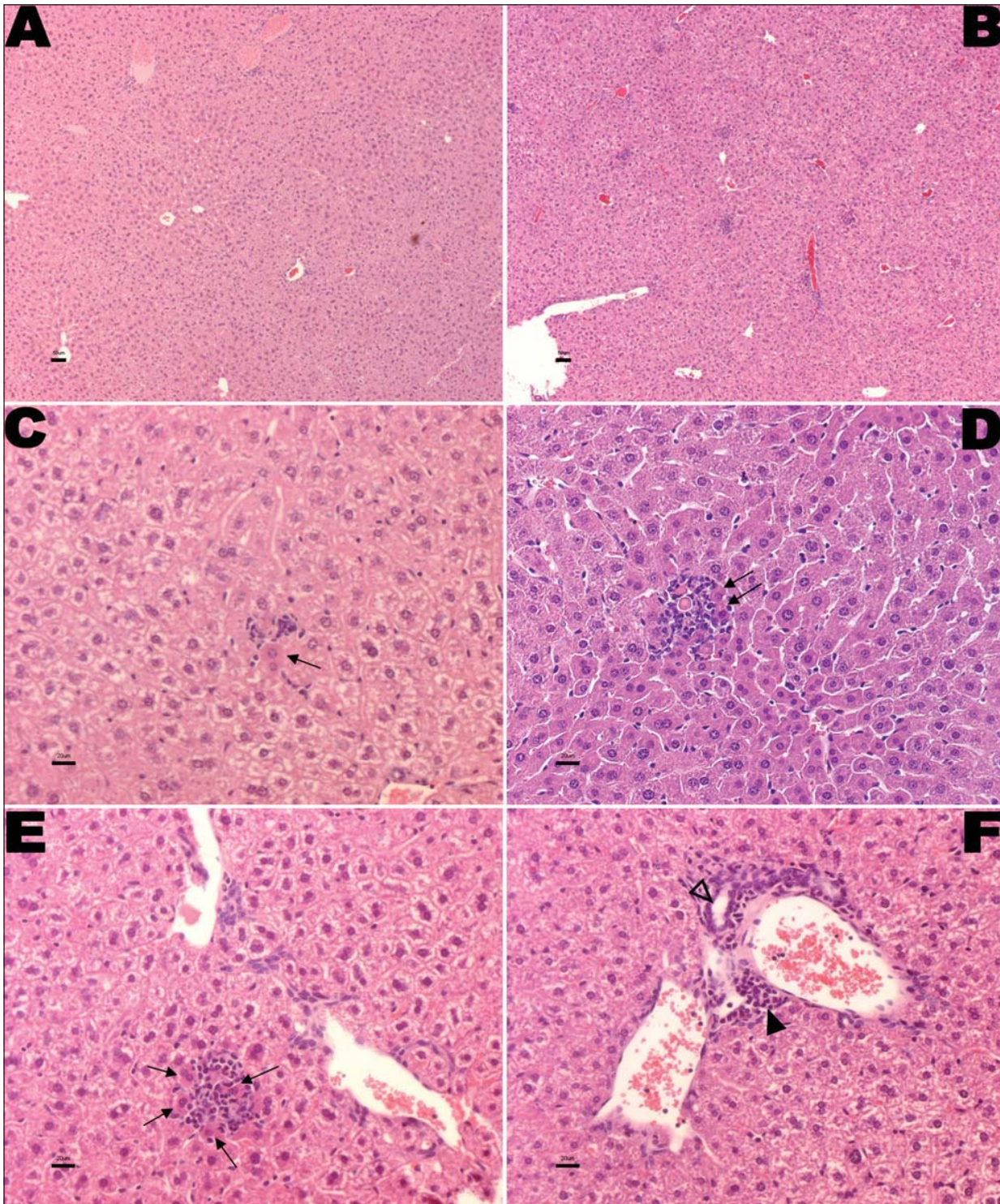


**Figure 1.** Photomicrographs of representative mouse liver sections. Hematoxylin and eosin stain; magnification 50 $\times$  (A, B), magnification 200 $\times$  (C through F), bar = 50  $\mu$ m. (A) Low-power view of the liver with infrequent lesions (category score, 1). Only occasional, small inflammatory infiltrates were observed in this liver section. (B) Low-power view of the liver with moderately frequent lesions (category score, 3). Note the multifocal distribution of lesions throughout the hepatic parenchyma. (C) Typical observation of a small inflammatory lesion (category score, 1), with apoptosis of individual hepatocytes (arrow) representative of mild hepatocyte damage (category score, 1). (D) Typical presentation of a moderately sized inflammatory lesion (category score, 2), with small aggregates of apoptotic hepatocytes (arrows) representative of a mild to moderate degree of hepatocyte damage (category score = 2). (E) Typical observation of a moderate-to-large-sized inflammatory lesion (category score, 3), with larger aggregates of apoptotic hepatocytes (arrows) representative of a moderate degree of hepatocyte damage (category score, 3). (F) Blood vessel showing bile duct proliferation (open arrowhead) and marked inflammatory infiltrate (solid arrowhead) representative of a perivascular inflammation score of 3.

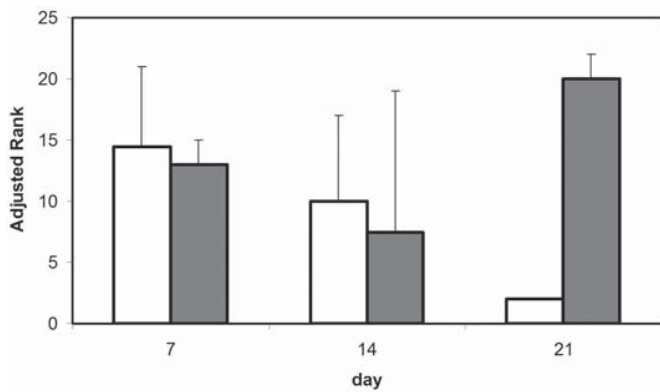


**Figure 2.** Median adjusted rank scores by day for L-NAME-treated (open bars) and untreated (shaded bars) *A. phagocytophilum*-infected mice in the initial experiment. Untreated mice (median, 20) had a trend ( $P = 0.10$ ) towards higher pathology rank on day 21 compared with L-NAME-treated mice (median, 2).

experiment only, as there were no significant differences in serum clinical chemistry parameters on days 7 and 14 between treatment groups in the initial experiment (day 21 serum clinical chemistry was not performed in either experiment).

## Discussion

The underlying mechanisms of pathophysiology and disease are not well understood for HGA, highlighting the need for a well-characterized, reproducible animal model. The initial observation of leukopenia in patients with intracellular infections of leukocytes misleads one to conclude that disease simply results from bacterial killing of host cells and subsequent inflammation. However, there is a marked discrepancy between the quantity of bacteria in blood and other tissues, degree of pancytopenia, and degree of histopathologic injury.<sup>18,36</sup> In HGA, 15-fold more cells are lost than can be accounted for by direct bacterial infection,<sup>1</sup> and cytopenias involve lineages that are not infected. These findings imply a role for host-mediated processes in pancytopenia, and by extension, injury to other tissues, such as liver. It is no surprise that disease and histopathologic evidence of tissue injury are linked to inflammatory reactions, because many investigators have demonstrated the production of inflammatory cytokines and chemokines or other biologically active products with *A. phagocytophilum* infections in vitro and in vivo.<sup>5,11,16,17</sup>

The role of immunity in disease with HGA continues to be investigated, and *A. phagocytophilum*-infected mouse models are valuable for understanding the pathogenetic mechanisms.<sup>4,7,22,23</sup> Mice reliably develop histopathologic lesions, cytokine responses, antibody responses, and bacterial loads very similar to those of

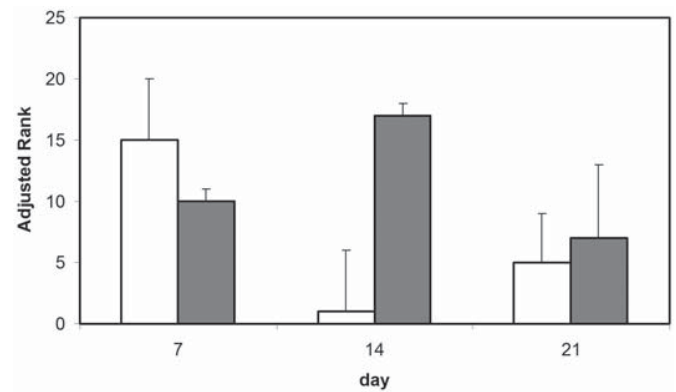


**Figure 3.** Median adjusted rank scores by day for L-NAME-treated (open bars) and untreated (shaded bars) *A. phagocytophilum*-infected mice in the replicate experiment. On day 7, L-NAME-treated mice (median, 15) had nearly significant ( $P = 0.0571$ ) higher rank scores than untreated mice (median, 10). At day 14, the trend was opposite, with untreated mice (median, 17) having nearly significant ( $P = 0.0571$ ) higher rank scores than L-NAME-treated mice (median, 1).

humans and susceptible domestic animals.<sup>7,18,22,36</sup> In the mouse model, genetic disruption of  $\text{IFN}\gamma$  production allows increased bacterial burden without a corresponding increase in histopathologic lesions, indicating that HGA is in part immune-mediated.<sup>23</sup> Immune effectors, such as NO, reactive oxygen species (ROS), and tumor necrosis factor  $\alpha$  ( $\text{TNF}\alpha$ ) are unable to control bacterial propagation.<sup>35</sup> However, loss of iNOS reduces the degree of histopathology in knockout mice early in infection, providing evidence that although ineffective at pathogen control, innate immunity is activated and contributes to tissue inflammation and injury.<sup>30</sup> Also noteworthy is that other innate immune effectors, such as ROS and  $\text{TNF}\alpha$ , contribute to histopathologic lesions, especially in the early stages of infection, before adaptive immunity is initiated.<sup>30</sup>

In this study, we hypothesized that hepatic histopathologic lesions and injury in *A. phagocytophilum*-infected C57BL/6 mice result from increased production of RNS after activation of macrophages by  $\text{IFN}\gamma$ . The data demonstrate that inhibition of iNOS was beneficial in limiting hepatic injury, most evident on day 14 when a milder degree of hepatic histopathology was observed concurrently with lower levels of urine and hepatic RNS. RNS are downstream products of the NO pathway, which has a variety of biologic functions, including modulation of inflammation and microbial growth.<sup>28</sup> There are 3 isozymes of NOS—brain and endothelial NOS, which are constitutive and produced in picomole amounts for short periods, and iNOS, which is produced in micromole amounts and is regulated at the level of transcription after stimulation of effector cells by cytokines and microbial prod-

**Table 3.** Reactive nitrogen species in liver and urine

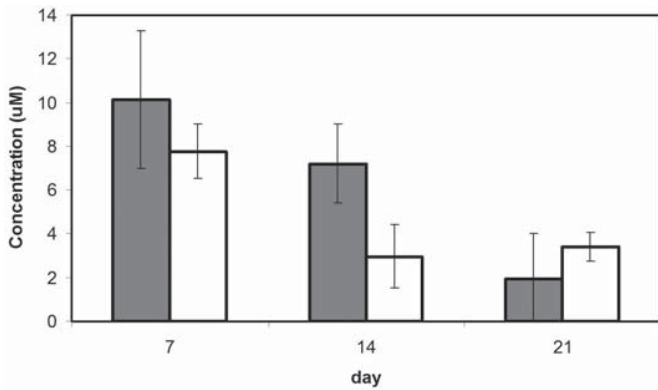
Sample source	Mice receiving untreated water	Mice receiving L-NAME-treated water	$P$
Liver, all mice, <sup>a</sup> day 14	7.09 ± 0.581	3.66 ± 0.794	0.0046
Liver, infected mice, <sup>b</sup> day 14	7.2 ± 0.901	4.2 ± 1.28	0.0215
Urine, all mice, day 14	527 ± 117	111 ± 8.85	0.0124
Urine, infected mice, day 14	527 ± 117	123 ± 11.0	0.0836
Urine, all mice, day 21	432 ± 123	185 ± 60.3	0.0885

Table includes only those comparisons found to be statistically significant or exhibiting a trend. All other comparisons measured were not significantly different from each other.

Data are presented as mean nitrate + nitrite concentration (in  $\mu\text{M}$ )/standardized mass:volume of liver and quantity of urine ± standard error of the mean.

<sup>a</sup>All mice refers to animals inoculated with uninfected HL-60 cells as well as HL-60 cells infected with *A. phagocytophilum*.

<sup>b</sup>Infected mice refers to animals inoculated with HL-60 cells infected with *A. phagocytophilum* only.



**Figure 4.** Measure of reactive nitrogen species (RNS) present in liver tissues by day for L-NAME-treated (open bars) and untreated (shaded bars) *A. phagocytophilum*-infected mice in the replicate experiment. Measurements of RNS in liver supernatants were significantly ( $P = 0.0215$ ) higher on day 14 for infected mice on untreated water compared with L-NAME-treated mice.

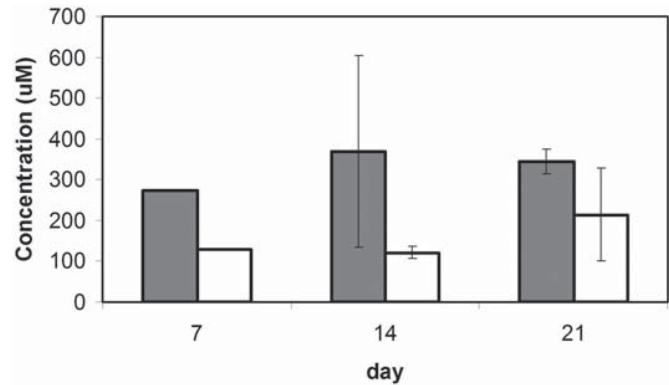


**Figure 5.** Measure of reactive nitrogen species (RNS) present in urine samples by day for L-NAME-treated (open bars) and untreated (shaded bars) *A. phagocytophilum*-infected mice in the replicate experiment. Differences in quantity of RNS from urine was similar to liver RNS results for day 14 infected mice, with a trend ( $P = 0.0836$ ) toward a greater quantity of urine RNS in untreated mice compared with L-NAME-treated mice. This finding was also similar for infected mice at day 21.

ucts, such as endotoxin.<sup>26,28</sup> The predominant mechanism of induction of iNOS and tissue damage occurs after induction of Th1 immunity and macrophage activation by IFN $\gamma$ . The consequent increase in NO and RNS leads to generation of peroxynitrites and other species that react with sulfhydryl groups to inactivate proteins, damage cellular DNA, and create protein nitrosylation in tissues.<sup>31,32,38</sup> The beneficial effects of NOS inhibition have also been shown with other bacterial infections.<sup>6,10,34</sup> This effect of NOS inhibition is especially beneficial when considering infections that trigger innate immune responses through IFN $\gamma$  and macrophage activation, and it indicates how important NO generation is for induction of tissue injury after innate immune system activation in HGA.

It is of interest that the effect of NOS inhibition in this study was seen at intervals after infection later than anticipated, suggesting an alteration in infection kinetics or additional involvement of adaptive immunity in the generation of tissue injury. Moreover, the difference in time to effect of NOS inhibition between the replicate experiments is also noteworthy. In the initial experiment, the effect occurred later than in the replicate, with peak pathology at day 21 compared to day 14, although NOS inhibitory effects were always most profound at time of peak pathology. The difference in disease kinetics could be due to bacterial infectivity or viability leading to delayed triggering of the innate immune response, among other possibilities. Even though rigorous cell culture conditions ensure standardized biology and behavior of infected cells over time, it is realistic to assume that there may be slight microbiologic differences in bacterial infectivity and kinetics between cell cultures used as inoculum in each experiment.

In the replicate experiment, there was more liver injury in day 7 L-NAME-treated mice, including increased ALT and glucose levels on day 14. It is possible that constitutive NOS isoforms that are inhibited by L-NAME in a dose-dependent manner are hepatoprotective.<sup>20,26,33</sup> L-NAME can reduce nitrate and nitrite levels in plasma and urine while concurrently increasing transaminase concentrations and histopathology that occurs with macrophage activation and local tissue inflammation.<sup>19</sup> Another side effect of L-NAME we noted was the increased glucose levels on day 14 in L-NAME-treated mice. This effect is known to be concentration-dependent and involves the regulation of insulin release.<sup>13</sup> We suspect that this phenomenon is due to the increased frequency

**Table 4.** Serum chemistry values for day 14 mice

Chemistry parameter	Mice receiving untreated water	Mice receiving L-NAME-treated water	<i>P</i>
Glucose (mg/dl)	260.3 $\pm$ 11.61	309.0 $\pm$ 18.36	0.0412
Alanine aminotransferase (U/l)	167.7 $\pm$ 58.73	405.0 $\pm$ 96.82	0.0531

Data are presented as mean  $\pm$  standard error of the mean.

of L-NAME water changes in the replicate experiment, which allowed for a greater total dose of L-NAME administered over 5 d compared to an every 2 to 3 d administration regimen. Regardless of these aberrations in ALT and glucose, the results of NOS inhibition observed here closely parallel those with infection in NOS-2 knockout mice with regard to hepatic histopathology and bacterial burden,<sup>30,35</sup> confirming the important role of NO in tissue injury with HGA and its inability to restrict bacterial propagation.

Although the absence of illness in infected mice is a limitation of the model because it imperfectly mimics natural disease, the mouse model is a refinement in the study of HGA because of the lack of clinical symptoms and animal distress. We used intraperitoneal inoculation of bacteria, an unnatural transmission mechanism that allows precise control of inoculum size and incurs much less distress to the mice than is associated with tick bite transmission. Theoretically, experimental infections transmitted by tick bite rather than intraperitoneal injection should mimic natural infection more closely, although mice still lack clinical signs when *A. phagocytophilum* is transmitted in this manner.<sup>9,14,15</sup> In horses, tick-bite transmission differs from intravenous transmission only in the incubation period,<sup>27</sup> suggesting that needle inoculation provides highly relevant data even compared with natural transmission, although contradictory results have also been reported.<sup>37</sup> Regardless, the murine model is effective for extending comprehension of HGA disease mechanisms.<sup>4,7,22,23,29</sup>

In conclusion, we demonstrate that C57BL/6 mice given L-NAME had reduced liver injury and inflammation, and this effect was mediated through immune mechanisms related to NO generation rather than to pathogen load in hepatic tissues. This abrogation of inflammation by L-NAME confirms the triggering of immunopathology with HGA, the role of macrophage activation in the disease process, and could help to generate novel

therapeutic strategies for *A. phagocytophilum* infections in humans and animals. Moreover, the induction of tissue injury via innate and adaptive immunity unrelated to pathogen load suggests that the typical approaches for vaccine development need to be considered carefully. The emerging recognition of HGA as an immunopathologic disease also indicates that novel therapies targeting reduced inflammation and innate immune response could be used to supplement the current anti-infective approach.

### Acknowledgments

The authors thank Nicole Barat for her technical assistance with experiments, Patricia Wilcox for histopathology processing, Baktiar Karim for assistance with photomicrographs, David Huso for the generous use of his histology camera, and the animal care staff of the Johns Hopkins University Research Animal Resources. This project was funded by an Institutional Research Grant through The Johns Hopkins University School of Medicine.

### References

- Bakken JS, Aguero-Rosenfeld ME, Tilden RL, Wormser GP, Horowitz HW, Raffalli JT, Baluch M, Riddell D, Walls JJ, Dumler JS. 2001. Serial measurements of hematologic counts during the active phase of human granulocytic ehrlichiosis. *Clin Infect Dis* 32:862–870.
- Bakken JS, Dumler JS, Chen SM, Eckman MR, Van Etta LL, Walker DH. 1994. Human granulocytic ehrlichiosis in the upper Midwest United States. A new species emerging? *J Am Med Assoc* 272:212–218.
- Banerjee R, Anguita J, Fikrig E. 2000. Granulocytic ehrlichiosis in mice deficient in phagocyte oxidase or inducible nitric oxide synthase. *Infect Immun* 68:4361–4362.
- Borjesson DL, Barthold SW. 2002. The mouse as a model for investigation of human granulocytic ehrlichiosis: current knowledge and future directions. *Comp Med* 52:403–413.
- Borjesson DL, Kobayashi SD, Whitney AR, Voyich JM, Argue CM, Deleo FR. 2005. Insights into pathogen immune evasion mechanisms: *Anaplasma phagocytophilum* fails to induce an apoptosis differentiation program in human neutrophils. *J Immunol* 174:6364–6372.
- Brennan RE, Russell K, Zhang G, Samuel JE. 2004. Both inducible nitric oxide synthase and NADPH oxidase contribute to the control of virulent phase I *Coxiella burnetii* infections. *Infect Immun* 72:6666–6675.
- Bunnell J, Triggiani ER, Srinivas SR, Dumler JS. 1999. Development and distribution of pathologic lesions are related to immune status and tissue deposition of HGE agent-infected cells in a murine model system. *J Infect Dis* 180:546–550.
- Chen S-M, Dumler JS, Bakken JS, Walker DH. 1994. Identification of a granulocytotropic *Ehrlichia* species as the etiologic agent of human disease. *J Clin Microbiol* 32:589–595.
- des Vignes F, Piesman J, Heffernan R, Schulze TL, Stafford KC III, Fish D. 2001. Effect of tick removal on transmission of *Borrelia burgdorferi* and *Ehrlichia phagocytophila* by *Ixodes scapularis* nymphs. *J Infect Dis* 183:773–778.
- Dowling RB, Newton R, Robichaud A, Cole PJ, Barnes PJ, Wilson R. 1998. Effect of inhibition of nitric oxide synthase on *Pseudomonas aeruginosa* infection of respiratory mucosa in vitro. *Am J Respir Cell Mol Biol* 19:950–958.
- Dumler JS, Triggiani ER, Bakken JS, Aguero-Rosenfeld ME, Wormser GP. 2000. Serum cytokine responses during acute human granulocytic ehrlichiosis. *Clin Diagn Lab Immunol* 7:6–8.
- Dumler JS, Walker DH. 2001. Tick-borne ehrlichioses: more of them, higher incidences, and greater clinical diversity. *Lancet Infect Dis* 0:21–28 (preview edition).
- Gentilcore D, Visvanathan R, Russo A, Chaikomin R, Stevens JE, Wishart JM, Tonkin A, Horowitz M, Jones KL. 2005. Role of nitric oxide mechanisms in gastric emptying of, and the blood pressure and glycemic responses to, oral glucose in healthy older subjects. *Am J Physiol Gastrointest Liver Physiol* 288:1227–1232.
- Hodzic E, Feng S, Fish D, Leutenegger CM, Freet KJ, Barthold SW. 2001. Infection of mice with the agent of human granulocytic ehrlichiosis after different routes of inoculation. *J Infect Dis* 183:1781–1786.
- Ijdo JW, Wu C, Telford SR III, Fikrig E. 2002. Differential expression of the p44 gene family in the agent of human granulocytic ehrlichiosis. *Infect Immun* 70:5295–5298.
- Kim HY, Rikihisa Y. 2000. Expression of interleukin 1 $\beta$ , tumor necrosis factor  $\alpha$ , and interleukin 6 in human peripheral blood leukocytes exposed to human granulocytic ehrlichiosis agent or recombinant major surface protein P44. *Infect Immun* 68:3394–3402.
- Klein MB, Hu S, Chao CC, Goodman JL. 2000. The agent of human granulocytic ehrlichiosis induces the production of myelosuppressing chemokines without induction of proinflammatory cytokines. *J Infect Dis* 182:200–205.
- Lepidi H, Bunnell JE, Martin ME, Madigan JE, Stuen S, Dumler JS. 2000. Comparative pathology and immunohistology associated with clinical illness after *Ehrlichia phagocytophila*-group infections. *Am J Trop Med Hyg* 62:29–37.
- Liaudet L, Rosselet A, Schaller MD, Markert M, Perret C, Feihl E. 1998. Nonselective versus selective inhibition of inducible nitric oxide synthase in experimental endotoxic shock. *J Infect Dis* 177:127–132.
- Liu TH, Robinson EK, Helmer KS, West SD, Castaneda AA, Chang L, Mercer DW. 2002. Does upregulation of inducible nitric oxide synthase play a role in hepatic injury? *Shock* 18:549–554.
- Lowenstein C. 2005. Personal communication.
- Martin ME, Bunnell JE, Dumler JS. 2000. Pathology, immunohistology, and cytokine responses in early phases of HGE in a murine model. *J Infect Dis* 181:374–378.
- Martin ME, Caspersen K, Dumler JS. 2001. Immunopathology and ehrlichial propagation are regulated by interferon-gamma and interleukin-10 in a murine model of human granulocytic ehrlichiosis. *Am J Pathol* 158:1881–1888.
- National Research Council. 1996. Guide for the care and use of laboratory animals. Washington (DC): National Academy Press.
- Olano JP, Wen G, Feng H-M, McBride JW, Walker DH. 2004. Histologic, serologic, and molecular analysis of persistent ehrlichiosis in a murine model. *Am J Pathol* 165:997–1006.
- Ou J, Carlos TM, Watkins SC, Saavedra JE, Keffer LK, Kim Y-M, Harbrecht BG, Billiar TR. 1997. Differential effects of nonselective nitric oxide synthase (NOS) and selective inducible NOS inhibition on hepatic necrosis, apoptosis, ICAM-1 expression, and neutrophil accumulation during endotoxemia. *Nitric Oxide Biol Chem* 1:404–416.
- Pusterla N, Leutenegger CM, Chae JS, Lutz H, Kimsey RB, Dumler JS, Madigan JE. 1999. Quantitative evaluation of ehrlichial burden in horses after experimental transmission of human granulocytic *Ehrlichia* agent by intravenous inoculation with infected leukocytes and by infected ticks. *J Clin Microbiol* 37:4042–4044.
- Salvemini D, Ischiropoulos H, Cuzzocrea S. 2003. Roles of nitric oxide and superoxide in inflammation. *Methods Mol Biol* 225:291–303.
- Scorpio DG, Akkoyunlu M, Fikrig E, Dumler JS. 2004. CXCR2 blockade influences *Anaplasma phagocytophilum* propagation but not histopathology in the mouse model of human granulocytic anaplasmosis. *Clin Diagn Lab Immunol* 11:963–968.
- Scorpio DG, von Loewenich FD, Bogdan C, Dumler JS. Tissue injury in the murine model of granulocytic anaplasmosis relates to host innate immune response and not pathogen load. *Ann NY Acad Sci*. Forthcoming.
- Szabo C, Ohshima H. 1997. DNA damage induced by peroxynitrite: subsequent biological effects. *Nitric Oxide Biol Chem* 1:373–385.

32. **Tarpey MM, Wink DA, Grisham MB.** 2004. Methods for detection of reactive metabolites of oxygen and nitrogen: in vitro and in vivo considerations. *Am J Physiol Regul Integr Comp Physiol* **286**:431–444.
33. **Taylor BS, Alarcon LH, Billiar TR.** 1998. Inducible nitric oxide synthase in the liver: regulation and function. *Biochemistry* **63**:766–781.
34. **Turco J, Liu H, Gottlieb SF, Winkler HH.** 1998. Nitric oxide-mediated inhibition of the ability of *Rickettsia prowazekii* to infect mouse fibroblasts and mouse macrophagelike cells. *Infect Immun* **66**:558–566.
35. **von Loewenich FD, Scorpio DG, Reischl U, Dumler JS, Bogdan C.** 2004. Frontline: control of *Anaplasma phagocytophilum*, an obligate intracellular pathogen, in the absence of inducible nitric oxide synthase, phagocyte NADPH oxidase, tumor necrosis factor, Toll-like receptor (TLR)2 and TLR4, or the TLR adaptor molecule MyD88. *Eur J Immunol* **34**:1789–1797.
36. **Walker DH, Dumler JS.** 1997. Human monocytic and granulocytic ehrlichioses. Discovery and diagnosis of emerging tick-borne infections and the critical role of the pathologist. *Arch Pathol Lab Med* **121**:785–791.
37. **Zeidner NS, Dolan MC, Massung R, Piesman J, Fish D.** 2000. Coinfection with *Borrelia burgdorferi* and the agent of human granulocytic ehrlichiosis suppresses IL-2 and IFN gamma production and promotes an IL-4 response in C3H/HeJ mice. *Parasite Immunol* **22**:581–588.
38. **Zhang J, Snyder SH.** 1992. Nitric oxide stimulates auto-ADP-ribosylation of glyceraldehyde-3-phosphate dehydrogenase. *Proc Natl Acad Sci U S A* **89**:9382–9385.